A METHOD OF DETERMINING THE GAS-PERMEABILITY PARAMETERS OF REINFORCED POLYMERS UNDER PYROLYSIS

V. M. Yudin, Yu. D. Khodzhaev, G. A. Ivanov, N. A. Levina, and V. S. Shpet

UDC 539.217.5

A method has been developed for determining gas-permeability parameters; results are presented for five different materials.

Damage occurs to the bonding agent at high temperatures, and the reinforced polymer releases gaseous decomposition products which penetrate to the surfaces through a system of pores. The resulting pressure differences tend to disrupt the stratified material if the gas flow is rapid. Also, the emerging decomposition products alter the heat-transfer conditions in the boundary layer and the composition of the medium within the shell.

One can determine the pressure distribution and the yield of decomposition products by solving the equation for the heating of reinforced plastics [1]; here one needs to have data on the gas-permeability parameters in relation to the degree of decomposition.

A modified Darcy equation [2] applies to the motion of the gas in the porous material over a fairly wide range of flow rates:

$$\operatorname{grad} p = \frac{\mu}{K}\mathbf{U} + \beta\rho_g U\mathbf{U}. \tag{1}$$

The first term on the right represents the pressure loss due to friction and the second term, the pressure loss due to dynamic effects, in particular, repeated sudden changes in cross-sectional area and sharp kinks. The inertial resistance coefficient β tends to zero at moderate flow rates, and (1) becomes an ordinary Darcy equation.

The gas-permeability coefficient K and the inertial-resistance coefficient are dependent on the porosity, temperature, and type of pores; the temperature dependence due to the thermal expansion is slight and may be neglected.

The pyrolysis in such a reinforced polymer increases the porosity, and so the gas-permeability parameters will be dependent on the initial structure of the material and on the degree of decomposition. If the true density alters only slightly, the porosity can be calculated from

$$m = m_0 + g_p \frac{\rho}{\rho_{p0}} \cdot \frac{\rho_{p0} - \rho_{pr}}{\rho_{p0}} \eta, \tag{2}$$

which is confirmed closely by experiment for hydrostatic conditions.

The initial porosity can also be determined by weighing with immersion or by microstructural examination, or again via

$$m_0 = 1 - g_p \frac{\rho}{\rho_{p0}} - (1 - g_p)\frac{\rho}{\rho_f}. \tag{3}$$

Zhukovskii Central Aerohydrodynamics Institute, Moscow. Translated from Inzhenerno-Fizicheskii Zhurnal, Vol. 29, No. 1, pp. 107-112, July, 1975. Original article submitted January 7, 1975.

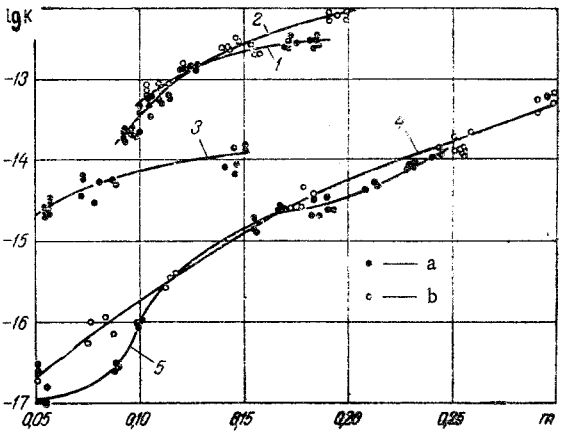

Fig. 1. Permeability of reinforced polymers in relation to porosity produced by pyrolysis: 1-5) materials; a and b) observed points.

The degree of decomposition on steady heating can be determined from the thermogravimetric curve, while the generalized Arrhenius equation can be applied to the nonstationary case [3].

Then the gas permeability can be determined via K(m) and β(m), which can be determined from tests on materials previously exposed to various temperatures provided that no other structural changes occur in the material, such as melting of the filler.

The gas permeability has been examined by a method based on quasistationary gas infiltration from the closed volume through the specimen. The pressure change in the volume is recorded, which serves to give K and β.

As the porosity is identical throughout the thickness δ (specimen uniformly pyrolyzed) and the gas moves in a one-dimensional fashion, (1) can be put as

$$-\frac{\partial p}{\partial x}=\frac{\mu}{K}U+\beta\rho_g U^2. \tag{4}$$

We substitute into (4) the infiltration rate from the equation of continuity for the gas flow:

$$\omega=F\rho_g U$$

and use the gas equation of state

$$p=\rho_g RT,$$

to get

$$-\frac{\partial p}{\partial x}=\frac{\mu}{K}\cdot\frac{RT}{F}\cdot\frac{\omega}{p}+\beta\frac{RT}{F^2}\cdot\frac{\omega^2}{p}. \tag{5}$$

We integrate (5) to get the pressure distribution in the specimen:

$$\frac{1}{2}(p^2-p_{atm}^2)=\left(\frac{\mu RT}{KF}\omega+\beta\frac{RT}{F^2}\omega^2\right)x. \tag{6}$$

The unknown gas flow rate through the specimen is determined by differentiation subject to T = constant for the gas within the chamber,

$$\omega=-\frac{V}{RT}\cdot\frac{dp}{dt}. \tag{7}$$

We substitute (7) into (6) and put x = δ to get

$$\frac{1}{2}(p^2-p_{atm}^2)=-\frac{\mu\delta V}{KF}\cdot\frac{dp}{dt}+\beta\frac{\delta V^2}{F^2RT}\left(\frac{dp}{dt}\right)^2. \tag{8}$$

Equation (8) defines the pressure change in the chamber on the assumption that (4) describes the gas infiltration into the specimen.

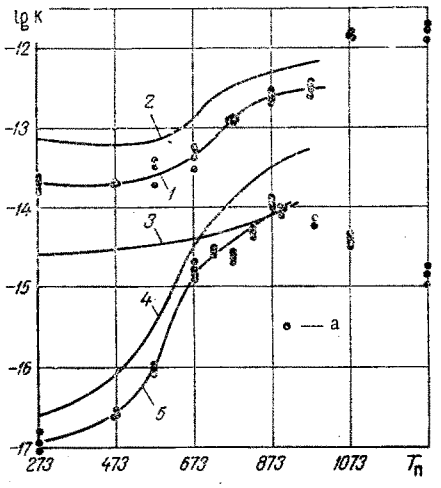

Fig. 2

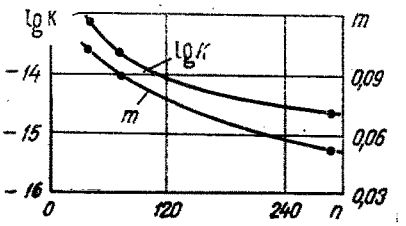

Fig. 3

Fig. 2. Permeability of reinforced polymers in relation to pyrolysis temperature: 1-5) materials; a) observed points.

Fig. 3. Permeability and initial porosity in relation to filler structure.

Then the gas-permeability parameters can be determined by fitting the observed pressure curve $p^e(t)$ to the curve given by (8); if we use the least-squares approach to fit the calculated curve to the observed $p(t)$, we get

$$\Delta = \left\{ \frac{1}{\bar{t}} \int_0^{\bar{t}} (p - p^e)^2 dt \right\}^{\frac{1}{2}}, \qquad (9)$$

where $\bar{t}$ is the run time.

The values of K and β that meet the restrictions $K \geq 0$ and $\beta \geq 0$ and also give a minimum in (9) are the desired gas-permeability parameters; the result for Δ_{min} allows one to judge how far the model fits the actual gas infiltration.

A program was written for the BÉSM-3M computer to perform the above calculations; (8) was solved numerically by iteration, which enabled us to obtain a solution even for $\beta = 0$. The values of $p^e(t)$ were given as a table, while values at intermediate points were determined by quadratic interpolation. The integral in (9) was calculated by the trapezium method. The minimum in (9) was determined by steepest descent. The restrictions on K and β were incorporated by gradient projection.

The measurements were made for the following materials: 1) TCP-K-9FA-14, 2) SK-9FA-MKT-5, 3) ASTT(δ)C_2-K-9FA, 4) TSP-FN-14, 5) ASTT(δ)-C_2-FH.

The first three materials are of fiberglass type with K-9FA phenol-organosilicon resin and fillers of TSP-14, MKT-5, and ASTT(δ)-C_2, while the fourth and fifth materials were phenol-furfural-formaldehyde plastics type FN with TSP-14 and ASTT(δ)-C_2 fillers.

The TSP-14 filler consisted of a cross-linked woven silica-fiber material with the following counts in weft and warp: $n_b = 9$ in the weft and $n_w = 8$ in the warp (both per cm), while MKT-5 was a multilayer silica fabric with three-dimensional weaving having counts of 8 and 5 in the above units, respectively, and ASTT(δ)-C_2 was an aluminoborosilicate satin-type woven glass material with counts of 22 and 13 in the above units.

Specimens of dimensions D = 28 mm and δ = 5 mm were cut from a sheet of the appropriate material; for each sheet we measured the density, bonding-agent content, and open porosity. The density and porosity were determined by weighing with immersion, while the bonding-agent content was determined by firing in air at 873°K.

The specimens were fired at various temperatures in the range 473-1273°K in a muffle furnace containing an inert amosphere; the heating rates were 30-40 deg/min, while the cooling was done was by switching off the furnace. The specimens were kept at set temperatures for 60 min. The specimens were weighted to 0.1 mg with analytical balances before and after pyrolysis.

The side surfaces of the fired specimens were covered with a silicate cement to give a uniform smooth film, which went with a lateral sealing device to prevent leakage of gas through the side surface, and also through any cracks between the layers; there was thus one-dimensional gas motion in the specimen. The infiltration area was determined with calibrated bushings as $0.314 \cdot 10^{-3}$ m^2. The volume of the sealed chamber was $V = 0.366 \cdot 10^{-3}$ m^3, and the initial pressure p_0 was 6 atm. The pressure was monitored by an MS-E2 manometer head (accuracy class 1.0) and was recorded by a single-point KSP-4 potentiometer recorder (accuracy class 0.25).

The data were processed as described above; the porosity produced by the pyrolysis was calculated from the actual weight loss:

$$m = m_0 + g_p \frac{\rho}{\rho_{p0}} \cdot \frac{G_0 - G}{g_p G_0}.$$

The gas-permeability parameters were defined via the gas-permeability coefficient on the assumption that there were no dynamic effects ($\beta = 0$); this gave good agreement between the observed and calculated curves for the pressure for each specimen. The mean values of Δ_{min} for the above materials were, correspondingly, 2, 2.8, 0.74, 0.96, and 0.83%. These results show that the Darcy equation in its usual form describes the gas infiltration closely for these materials. The Δ_{min} for the first two materials were somewhat larger than those for the others, and these materials had higher permeability, which indicated the onset of dynamic effects. However, these were still small and negligible.

Figures 1 and 2 show the results as the permeability coefficient as a function of porosity and pyrolysis temperature. They also show average curves and data for each specimen. At temperatures up to 973°K (fiberglass materials containing alumoborosilicate glass) or 1073°K (silica fillings) there was a regular increase in the permeability, whereas at higher temperatures there was deviation from this trend, with the permeability coefficient tending to decrease for the first group of materials and increase for the second. This is clear from the results of Fig. 2 for the two corresponding materials. Microstructural examination of the fired specimens showed that the filaments had broken in the silica fillers under these conditions, which produced additional paths for gas passage, whereas the aluminoborosilicate filler material showed some melting in the fibers, which had closed some of the pores.

Figure 3 shows the gas-permeability coefficient for materials containing K-9FA phenol-organosilicon bonding agent in relation to the structure parameter, which is the product of the number of fibers per cm in the warp and weft. A similar relationship was observed also for the initial porosity.

NOTATION

x, coordinate; p, pressure; μ, dynamic viscosity; U, interstitial velocity; K, gas-permeability coefficient; β, inertial-resistance coefficient; m, porosity; η, degree of polymer decomposition; g_p, weight content of polymer; R, gas constant; F, infiltration area; V, chamber volume; ω, mass gas flow rate; n_b, n_w, number of threads per 1 cm on warp and weft; n, fabric structure parameter; ρ, ρ_f, ρ_g, densities of material, filler, and gas; ρ_{p0}, ρ_{pr}, ρ_p, densities of monolithic polymer, apparent density of residue and of polymer during destruction. Subscripts: 0 denotes initial; atm denotes atmospheric.

LITERATURE CITED

1. V. M. Yudin, "Heat conduction in glass plastics," Tr. Tsentr. Aéro-Gidrodinam. Inst., No. 1267 (1970).
2. L. Green Jr. and P. Duwez, J. Appl. Mech, 18; Trans. ASME, 73, 39 (1951).
3. G. E. Vishnevskii and G. E. Yudin, Inzh.-Fiz. Zh., 16, No. 5 (1969).